MOLECULAR AND CELLULAR BIOLOGY, June 1987, p. 2155–2164
0270-7306/87/062155-10$02.00/0

Vol. 7, No. 6

Isolation and Characterization of Temperature-Sensitive RNA Polymerase II Mutants of *Saccharomyces cerevisiae*

HOWARD J. HIMMELFARB, ELIZABETH M. SIMPSON, AND JAMES D. FRIESEN*

Department of Medical Genetics, University of Toronto, Toronto, Ontario, Canada M5S 1A8

Received 21 November 1986/Accepted 16 March 1987

Three independent, recessive, temperature-sensitive (Ts^-) conditional lethal mutations in the largest subunit of *Saccharomyces cerevisiae* RNA polymerase II (RNAP II) have been isolated after replacement of a portion of the wild-type gene (*RPO21*) by a mutagenized fragment of the cloned gene. Measurements of cell growth, viability, and total RNA and protein synthesis showed that *rpo21-1*, *rpo21-2*, and *rpo21-3* mutations caused a slow shutoff of RNAP II activity in cells shifted to the nonpermissive temperature (39°C). Each mutant displayed a distinct phenotype, and one of the mutant enzymes (*rpo21-1*) was completely deficient in RNAP II activity in vitro. RNAP I and RNAP III in vitro activities were not affected. These results were consistent with the notion that the genetic lesions affect RNAP II assembly or holoenzyme stability. DNA sequencing revealed that in each case the mutations involved nonconservative amino acid substitutions, resulting in charge changes. The lesions harbored by all three *rpo21* Ts^- alleles lie in DNA sequence domains that are highly conserved among genes that encode the largest subunits of RNAP from a variety of eucaryotes; one mutation lies in a possible Zn^{2+} binding domain.

Transcription in eucaryotic cells is carried out by three functionally and structurally distinct nuclear RNA polymerase (RNAP) types. RNAP I, II, and III (or A, B, and C) synthesize rRNA, mRNA, and 5S and tRNA, respectively, and can be distinguished on the basis of their subunit composition, nuclear location, cofactor requirements, and sensitivity to the mycotoxin α-amanitin (for a review, see reference 45). Eucaryotic nuclear RNAPs have a similar basic subunit structure, consisting of 2 nonidentical large subunits ($M_r > 100$) and 7 to 12 smaller polypeptides (45).

The structure of the large polymerase subunits has been conserved through evolution. Immunological cross-reactivity studies have shown that the large polypeptides of *Saccharomyces cerevisiae* RNAP II share a number of antigenic determinants with the analogous subunits from wheat germ, *Artemia salina*, *Drosophila melanogaster*, and calf thymus (6, 8, 22, 56). The large subunits of yeast RNAP I, II, and III are also antigenically related (8). Recent gene cloning (10, 24, 44, 50) and DNA sequence comparisons (1, 3, 7; J. Corden, personal communication) indicate that this conservation of antigenic determinants is a reflection of conserved amino acid sequence domains. Thus, six blocks of sequence homology have been identified in the genes encoding the largest subunits of yeast RNAP I, II, and III (1; S. Memet and J.-M. Buhler, personal communication), mouse RNAP II (J. Corden, personal communication), and *Vaccinia* virus RNAP (7). Three of these have also been identified in partial DNA sequence data from the amino terminus of the *Drosophila* gene (3). Five of the six homology regions can be found (with their colinear order maintained) in the *Escherichia coli* β′ gene, which encodes the largest subunit of procaryotic RNAP (41). Taken together, these data suggest that the three eucaryotic RNAPs had a common evolutionary origin and arose after triplication of the genes encoding the large subunits of the enzyme.

The central role of RNAP II in the regulation of gene expression makes it an important subject for mutational analyses, particularly in a genetically tractable organism such as *S. cerevisiae*. RNAP subunit mutations can be used to study the regulation of polymerase biosynthesis (19) and to reveal a function for evolutionarily conserved sequence domains. Conditional lethal mutants also provide hosts for the selection of unlinked pseudorevertants; such suppressor mutations may identify functional interactions between *RPO21* and other RNAP subunits or transcription factors.

In cultured mammalian cells (9, 23, and references therein) and in *D. melanogaster* (17), resistance to the mycotoxin α-amanitin, which acts as a specific inhibitor of RNAP II transcription when used at low concentrations (26, 31, 53), has been used to isolate mutations in the largest subunit of the enzyme. Resistance to α-amanitin has not been a useful marker for the largest RNAP II subunit gene in *S. cerevisiae* because cells are relatively impermeable to the toxin (13) and the purified yeast enzyme is 100- to 500-fold more resistant to α-amanitin than is RNAP II isolated from higher eucaryotes (49, 53). To begin a genetic study of RNAP II in *S. cerevisiae*, we have mutagenized a DNA segment encoding a portion of the largest subunit (alternatively named *RPO21* [24] or *RPB220* [44]) and have directed mutations to the native chromosomal locus by transformation and homologous recombination. Here we present a characterization of three such mutants that lead to a temperature-sensitive (Ts^-), conditional lethal growth defect in vivo.

MATERIALS AND METHODS

Strains, plasmids, and growth conditions. The *S. cerevisiae* strains used in this study are described in Table 1. *E. coli* K-12 JF1754 (*hsdR* Lac^- Gal^- *metB leuB hisB*) was used as the bacterial host. pMS57 (obtained from C. J. Ingles, University of Toronto, Ontario) consists of an *Eco*RI-*Bgl*II DNA fragment comprising the amino-terminal 3,402 base pairs of the *RPO21* coding sequence (1) carried on a derivative of pEMBL8 (12) with a 1.1-kilobase (kb) *Hin*dIII DNA fragment containing the yeast *URA3* gene inserted into the polylinker. Plasmids prpo21-1, prpo21-2, and prpo21-3 were all derived from pMS57 after nitrosoguanidine mutagenesis (15) and in vivo Ts^- mutant selection as described in Results. pJH121 consists of two *Eco*RI DNA fragments of

* Corresponding author.

TABLE 1. Strain descriptions[a]

Strain	Description
SC252	*MAT*α *ura3-52 leu2-3,-112 ade1*; obtained from D. Thomas, National Research Council, Biotechnology Research Institute, Montreal, Quebec
SR25-1A	*MAT***a** *ura3-52 his4-912*; obtained from S. Roeder, Yale University, New Haven, Conn.
YHP227	*MAT***a** *ura3-52 his4-912* prpo21-1::*URA3*; transformant of SR25-1A with prpo21-1 integrated at *RPO21* (SR25-1A::prpo21-1::*URA3*)
YHP225	*MAT***a** *ura3-52 his4-912 rpo21-1*; Ts$^-$, 5-FOA-resistant outgrowth from YHP227
YHP214	*MAT***a** *ura3-52 his4-912 rpo21-2*; Ts$^-$, 5-FOA-resistant outgrowth from SR25-1A::prpo21-2::*URA3* transformant
YHP218	*MAT***a** *ura3-52 his4-912 rpo21-3*; Ts$^-$, 5-FOA-resistant outgrowth from SR25-1A::prpo21-3::*URA3* transformant
YHP568	*MAT***a** *his4-912*; transformant of SR25-1A with pJH18 integrated at *URA3*
YHP569	*MAT***a** *his4-912 rpo21-1*; transformant of YHP225 with pJH18 integrated at *URA3*
YHP570	*MAT***a** *his4-912 rpo21-2*; transformant of YHP214 with pJH18 integrated at *URA3*
YHP571	*MAT***a** *his4-912 rpo21-3*; transformant of YHP218 with pJH18 integrated at *URA3*

[a] For a description of the plasmids, see Materials and Methods.

7.0 and 1.7 kb (24) cloned from the *RPO21* locus and inserted in the genomic orientation into the unique *Eco*RI site of pint2 (42). pint2 is an *E. coli*-yeast shuttle vector which is stably maintained as an episome in *S. cerevisiae* as a result of the presence of a functional centromere (*CEN3*) and origin of replication (*ARS1*) and which carries the selectable *URA3* yeast gene. pJH18 (from J. Haber, Brandeis University, Waltham, Mass.) is pBR322 with the *URA3* gene carried on a 1.1-kb *Hin*dIII DNA fragment. pJH124 was constructed by inserting a 7.0-kb *Eco*RI *RPO21* DNA fragment and a 1.1-kb *Hin*dIII *URA3* DNA fragment into the polylinker of pUC8 (55).

Transformation of *S. cerevisiae* after treatment with lithium acetate was performed as described (25). For mutant isolation and marker-rescue experiments requiring a high efficiency of transformation, yeast spheroplasts were prepared as described (21). For the marker-rescue experiments, gapped, linear plasmids were gel purified, after digestion with the appropriate restriction endonuclease(s), by extraction from low-melting-point agarose gels (33). Growth and transformation of *E. coli* was essentially as described previously (33).

Yeast media were prepared as described by Klapholz and Esposito (28). Minimal defined medium consisted of 0.7% yeast nitrogen base without amino acids (Difco Laboratories) and 2% glucose supplemented only with the amino acids and the four nitrogenous bases absolutely required. Complete defined medium consisted of minimal defined medium supplemented with all 20 amino acids and nitrogenous bases. Omission medium was complete defined medium lacking one or more amino acids or nitrogen bases. 5-Fluoro-orotic acid (5-FOA) medium was prepared as described (4) with 5-FOA added to a concentration of 1 mg/ml. 5-FOA solid medium was found to be stable for no longer than 1 week at 4°C in the dark. All defined liquid media were buffered to pH 5.8 with sodium succinate (ca. 10 g of succinic acid and 6 g of sodium hydroxide per liter).

DNA and RNA manipulations. Enzymes and reagents were purchased from Boehringer Mannheim Canada, Bethesda Research Laboratories, Inc., New England Nuclear Corp., Bio-Rad Laboratories, and New England BioLabs, Inc. DNA manipulations were done by standard methods described previously (33). Yeast DNA was purified as described earlier (11). DNA blotting, nick translation, and nucleic acid hybridization have been described previously (33). Mutant integrated prpo21 plasmids were recovered from yeast cells by digesting total genomic DNA with *Xba*I (the enzyme used to linearize the plasmids before integration; see below) and then ligating at a low DNA concentration (25 μg/ml) and T4 DNA ligase concentration (0.1 U/μg), followed by transforming into *E. coli* with selection for ampicillin resistance.

Sequencing of the three *rpo21* mutants was done by the dideoxy method (48). The *Bal*I-to-*Tth*III1 fragment (base pairs +98 to +1088, relative to the start of the coding sequence) from prpo21-1, prpo21-2, and prpo21-3 was cloned in its entirety into M13mp18 (58). Oligonucleotides (18-mer) complementary to regions approximately 250 base pairs apart on the *RPO21* fragment or to the flanking M13 DNA (19-mer) were synthesized by using an Applied Biosystems model 380B DNA synthesizer. Oligonucleotide purification was done by gel electrophoresis. Mutant assignment was done on the basis of the agreement of the sequence data from at least four independent M13 clones.

Measurements of growth, viability, and total RNA and protein synthesis rates. Growth was measured by nephelometry at 600 nm with a Zeiss PMQ-2 spectrophotometer. A shift from the permissive (30°C) to restrictive (39°C) temperature was accomplished by adding an equal volume of minimal medium, prewarmed to 48°C, to cells growing exponentially at 30°C, followed immediately by incubation at 39°C. Wild-type *RPO21* strains were subcultured during RNA and protein pulse-labeling experiments to ensure continued exponential growth; the optical density at 600 nm of these cultures was not permitted to exceed 2.0 during an experiment. Kinetics of death were determined by removing samples of cells at various times after a temperature shift. Cell suspensions were then sonicated to disrupt cell clumps by using a Heat Systems Co.-Ultrasonics, Inc. sonifier cell disrupter model W140D at an output of 50 to 70 W with a standard microtip. Sonication time was 30 to 45 s (10-s intervals with 30-s cooling periods in wet ice). Cells were then diluted in sterile distilled water, and samples were spread on YPDA (1% yeast extract, 2% Bacto-Peptone, 2% glucose, and 0.004% adenine) plates and were incubated at 30°C for 3 days to permit colony development.

Total cellular protein was labeled with L-[^{35}S]methionine (50 μCi/ml, 71,000 Ci/mmol). Cells were labeled in minimal medium for 5 min with vigorous agitation, poured over crushed ice containing 0.2 mg of L-methionine per ml, frozen in dry ice, and stored at −80°C. Cell extracts were prepared as described previously (36). Protein concentration was determined by the method of Bradford (5) by using Bio-Rad protein assay dye reagent concentrate. The incorporation of radioactivity into cells was quantitated as follows. Samples (3 μl) of cell extract were precipitated with 2 ml of 5% trichloroacetic acid in the presence of 100 μg of bovine serum albumin per ml (fraction V) and boiled for 5 min; after cooling, the trichloroacetic acid-precipitable material was

collected on Whatman GF/C filters that had been presoaked in an aqueous solution of 1% methionine; dried filters were counted in Econofluor, using a United Technologies Packard MINAXI Tri-Carb 4,000 series scintillation counter.

Total cellular RNA was radioactively labeled with [5-^{3}H]uracil (50 μCi/ml, 26 Ci/mmol). Cells were labeled in minimal medium for 5 min with vigorous agitation, poured over crushed ice, frozen in dry ice, and stored at −80°C. Before RNA extraction, all samples were mixed with a constant volume of a YHP568 culture (wild type) that had been continuously labeled with carrier-free [^{32}P]orthophosphoric acid (2.5 μCi/ml) during at least three generations of exponential growth. Sufficient ^{32}P-labeled cells were added so that the ^{32}P/^{3}H ratio was approximately 1:10 after RNA extraction. Total cellular RNA was prepared as described previously (20). Variation in RNA extraction efficiency among the samples was monitored by measuring the counts per minute of ^{32}P present in each RNA preparation. Changes in nucleotide pool sizes occurring during the experiment were not determined. Radioactivity incorporated into RNA was measured by adding 3-μl samples of an aqueous RNA solution to 10 ml of Aquasol II and counting as described above. RNA synthesis rates shown (see Fig. 3B) are expressed as the counts per minute of [^{3}H]uracil incorporated per the optical density at 600 nm of the culture, after correcting for differences in RNA extraction efficiency.

RNA synthesis was measured in permeabilized cells by using the run-on transcription assay described by Elion and Warner (13), with the following modification. The concentration of [α-^{32}P]UTP was 0.1 mCi/ml, instead of 1.0 mCi/ml; unlabeled UTP was added so that the final concentration of UTP was unchanged (0.3 μM). In experiments in which it was necessary to inhibit RNAP II transcription, α-amanitin (75 μg/ml) was added to the reaction. The assay temperature was 23°C.

In vitro random transcription reactions specific for RNAP II or RNAP I and RNAP III polymerase activities were performed by using S100 cell extracts as described previously (46). The reaction mixture to measure RNAP II activity contained 50 μg of r(C)$_n$ per ml and 0.5 mg of crude protein extract per ml in 70 mM Tris hydrochloride (pH 8.0), 3 mM $MgCl_2$, 5 mM dithiothreitol, 40 mM $(NH_4)_2SO_4$, and 0.5 mM GTP. RNAP I and III reaction mixtures contained 50 μg of d(I-C)$_n$ per ml and 0.5 mg of crude protein extract per ml in 70 mM Tris hydrochloride (pH 8.0), 5 mM $MgCl_2$, 5 mM dithiothreitol, 1 mM CTP, and 0.5 mM GTP. Radioactive [8,5′-^{3}H]GTP (25 to 50 Ci/mmol) was added to all reaction mixtures to a final concentration of 5 μCi/ml. Unless otherwise stated, 100-μl reaction volumes were incubated at 30°C for 20 min and then were spotted onto Whatman DE-81 filter disks. Filters were washed six times with 0.5 M Na_2HPO_4, were washed once each with water, ethanol, and ether, and then were dried. Radioactivity incorporation was measured by immersing each filter in 10 ml of Econofluor and counting as described above.

Each experiment (except for RNA pulse-labeling) was done at least twice with similar results. The data presented here were from single experiments; the reproducibility of the data was within 10%.

RESULTS

Generation of Ts⁻ rpo21 mutants. In *S. cerevisiae*, a highly efficient system of DNA transformation and homologous recombination allowed cloned DNA fragments modified in vitro to replace sequences at the homologous locus on the yeast chromosome. A *RPO21* gene fragment containing the coding region for the amino-terminal two-thirds of the polypeptide (Fig. 1A) was cloned into a yeast-integrating plasmid marked with *URA3* (pMS57; see Materials and Methods). pMS57 was mutagenized with nitrosoguanidine, as referred to in Materials and Methods, to generate a pool of randomly mutagenized plamids. A unique *Xba*I site at position +2531, relative to the translation start site (1), was used to linearize the plasmid before transformation. A double-strand cut enhanced the frequency of homologous recombination 100- to 1,000-fold and directed integration at the site of the cut (40) (Fig. 1A), in this case to the *RPO21* locus rather than to

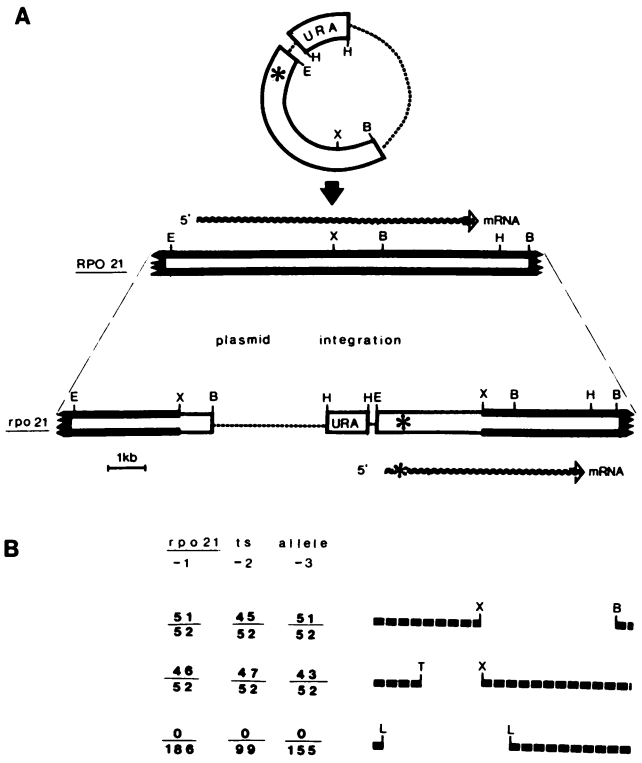

FIG. 1. Generation and mapping of *rpo21* Ts⁻ mutations. (A) Recombination event that occurs during generation of *rpo21* Ts⁻ mutants. Abbreviations: B, *Bgl*II (for clarity, only two sites are indicated); E, *Eco*RI; H, *Hin*dIII; X, *Xba*I. Open rectangles represent yeast DNA, and the thin, dashed line represents pEMBL8 sequences. Thick-lined rectangles represent chromosomal DNA, and thin-lined rectangles represent yeast sequences carried on the integrating plasmid (pMS57). The wavy lines represent the approximate position of the *RPO21* transcript. An asterisk marks the site of a *rpo21* mutation. The *URA3* gene carried on the plasmid is indicated. Recombination was directed by linearization of pMS57 at the *Xba*I site (position +2531). (B) Mapping *rpo21* Ts⁻ mutations. Abbreviations: B, *Bgl*II (+4445); L, *Bal*I (+96 and +3321); T, *Tth*111I (+1089); X, *Xba*I (+2531); the position(s) of endonuclease cleavage sites, relative to the start of the *RPO21* coding sequence, are given above in parentheses (1). -1, -2, and -3 signify *rpo21* mutant allele numbers. The thick, dashed lines represent *RPO21* DNA fragments carried on the plasmid pJH124 that had been purified from low-melting-point agarose gels before transformation of YHP225 (*rpo21-1*), YHP214 (*rpo21-2*), and YHP218 (*rpo21-3*). The numbers to the left of each line summarize the results of transformation of *rpo21* Ts⁻ strains with the indicated fragment. The denominator gives the total number of Ura⁺ transformants screened, while the numerator indicates the number of these that were Ts⁺.

the *URA3* locus. Plasmid integration at *RPO21* resulted in a partial duplication of the *RPO21* gene with the single intact gene containing plasmid-derived and chromosomal sequences (Fig. 1A). Any nitrosoguanidine-induced recessive mutations in plasmid sequences that are resolved in the intact *RPO21* gene can be expressed in these Ura$^+$ transformants.

Approximately 10,000 Ura$^+$ SC252 (*Matα ura3-52*) (only relevant genotypes are given; for a complete description, see Table 1) transformants were selected at 23°C and then replica plated to test for growth at 36.5°C to detect Ts$^-$ colonies. Complex-rich (YPDA) medium was used to avoid Ts$^-$ *ura3* mutants. The frequency of Ts$^-$ transformants was 10^{-2} and, surprisingly, was similar in separate experiments when the transforming DNA had not been mutagenized or in a mock transformation without any transforming DNA. This high frequency of transformation-induced temperature sensitivity is apparently caused by the spheroplasting transformation procedure itself (51). As described below, we found that most transformation-induced Ts$^-$ cells can be identified on the basis of the genetic instability of their Ts$^-$ phenotype.

A total of 104 recessive Ts$^-$ transformants were subcultured serially by restreaking on uracil-omission solid medium agar for approximately 200 generations at 23°C, testing periodically for growth at 36.5°C. Only five transformants were stably Ts$^-$. Plasmid DNA integrated at the *RPO21* locus was then recovered from one of these five mutants (called Ts1) (see Materials and Methods). This was done for two reasons. First, if a plasmid were recovered which transforms cells to a Ura$^+$ Ts$^-$ phenotype, then the Ts$^-$ phenotype of the original transformant must have been due to the integrated, mutated *RPO21* plasmid sequences and not to an unrelated transformation-induced event. Second, the recovered, mutated plasmid DNA would then be available for DNA sequencing.

DNA blot-hybridization analysis of mutant Ts1 (data not shown; for an example, see reference 39) indicated that several plasmids had integrated tandemly and adjacent to the *RPO21* gene. Although the Ts$^-$ phenotype depends only on mutation of the one plasmid-derived DNA copy that had recombined into the chromosomal *RPO21* gene, the adjacent, tandemly integrated plasmids that had entered the chromosome would also be recovered in the population of ampicillin-resistant *E. coli* colonies derived from *Xba*I-digested yeast chromosomal DNA. These latter plasmids in principle could carry either wild-type or mutated *RPO21* sequences. Therefore, six independent plasmids isolated from *E. coli* that had been transformed with DNA from mutant Ts1 were tested for their ability to transform strain SR25-1A (*MAT***a** *ura3-52*) to the Ura$^+$ Ts$^-$ phenotype. Again, plasmids were linearized with *Xba*I before the transformation to target integration to the *RPO21* locus. Only one of the six plasmids tested (prpo21-1) yielded a high frequency of Ts$^-$ colonies among the Ura$^+$ transformants; 50% of the Ura$^+$ transformants were Ts$^-$, indicating that in one half of the integration events, the mutated portion of the plasmid-derived gene was now contiguous with the intact *RPO21* gene. Since prpo21-1 was recovered from colony-purified *E. coli*, we suggest that this observed recovery of less than 100% Ts$^-$ colonies among all Ura$^+$ transformants was due to exonucleolytic or repair events that occur during plasmid integration. The ability to transform yeast at high frequency to a Ts$^-$ phenotype with plasmid prpo21-1 confirmed that this DNA contains a mutation in the *RPO21* sequence. The other five plasmids gave only background numbers of Ts$^-$ colonies (frequency, 10^{-2}) and thus were derived from wild-type plasmids that integrated adjacent to prpo21-1 in the original Ts$^-$ transformant Ts1.

Next it was determined whether the recessive Ts$^-$ phenotype displayed by any of the remaining four original SC252 (Ura$^+$ Ts$^-$) transformants was due to a mutation allelic to *rpo21-1*. A complementation assay using the Ts$^-$ phenotype of YHP227 (*MAT***a** *ura3-52* prpo21-1::*URA3*; Table 1) as a marker demonstrated that only two of the remaining four original transformants were Ts$^-$ *rpo21* mutants (i.e., failed to complement *rpo21-1*). Plasmid DNA (prpo21-2 and prpo21-3) was recovered from these cells as described above for prpo21-1. The other two Ts$^-$ transformants were probably the result of a transformation-induced Ts$^-$ event that did not involve *RPO21*.

A congenic set of strains (YHP225, YHP214, and YHP218) carrying the three *rpo21* mutations was generated by first transforming strain SR25-1A (*MAT***a** *ura3-52*) with prpo21-1, prpo21-2, and prpo21-3 DNA. To derive stable *rpo21* Ts$^-$ alleles, single-copy Ura$^-$ Ts$^-$ recombinants (Table 1) were then selected by growth in the presence of 5-FOA, as described in Materials and Methods. DNA blot-hybridization analysis of these 5-FOA-resistant outgrowths confirmed that pEMBL, *URA3*, and the partial *RPO21* duplication had been lost (data not shown). As expected, the Ts$^-$ phenotype of these *rpo21* strains can be complemented by a wild-type *RPO21* gene carried on the episomal plasmid pJH121 (data not shown).

The parental strain SR25-1A formed colonies on solid medium at temperatures up to 41°C; at 39°C, it grew with a generation time of 2.5 h in minimal medium (Fig. 2A). The Ts$^-$ phenotype of SR25-1A strains carrying an *rpo21* mutant allele was leaky at 36.5°C, but all three *rpo21* mutants were Ts$^-$ lethal at 39°C (Fig. 2B). Therefore 39°C was chosen as the nonpermissive temperature for all subsequent experiments.

Physiological changes due to rpo21 mutations. (i) Growth rate and viability. Growth of *rpo21* mutant cells, as measured by an increase in optical density, continued at rates similar to that of the wild type for approximately one generation time (2.5 h) after a temperature shift (Fig. 2A). After that time, the growth rate decreased slowly for strains YHP569 (*rpo21-1*) and YHP571 (rpo21-3) and slightly more rapidly for YHP570 (rpo21-2) (Fig. 2A). All three mutant strains began to die after about 8 h at 39°C (Fig. 2B). Comparison of Fig. 2A and B reveals that YHP569 (*rpo21-1*) and YHP571 (*rpo21-3*) strains were more thermotolerant than YHP570 (*rpo21-2*) was; both showed an extended period of growth and prolonged cell viability after the temperature shift.

(ii) Protein synthesis. The rate of synthesis of an individual protein species may be used as an indirect measure of the steady-state concentration of its mRNA within the cellular pool and, thus, as an indication of the relative synthesis rate of its mRNA. The rate of cellular protein synthesis was measured by pulse-labeling cells with L-[^{35}S]methionine at intervals after a temperature shift as described in Materials and Methods. This temperature shift (30 to 39°C) is sufficient to induce a heat shock response (32). In yeast cells, the heat shock response is mediated by a transient change in RNAP II promoter selection, leading to the induction of a variety of heat shock proteins and repression of synthesis of most other cellular proteins (for a review, see reference 32). This transcriptional shift is reflected by a transient drop in the rates of protein synthesis (Fig. 3A; 38), reaching a minimum after approximately 90 min and recovering to 70 to 80% of preshift levels by 4 h. As might have been expected from measurements of growth rate up to 4 h after a shift (Fig. 2A),

all three mutants show a wild-type heat shock response. Comparison of the proteins synthesized by sodium dodecyl sulfate-polyacrylamide gel electrophoresis (data not shown) indicates that at least at this level of resolution, there was no dramatic difference between the mutants and wild type. Between 4 and 8 h after the temperature shift, there was a marked decrease in the rates of protein synthesis in the mutants relative to the wild type. As described in Materials and Methods, cultures of YHP568 (*RPO21*) were subcultured into prewarmed medium at intervals during this experiment and during the RNA pulse-labeling experiment described below to ensure continued exponential growth.

(iii) RNA synthesis. Rates of total cellular RNA synthesis after a shift were measured by pulse-labeling cells with [^{3}H]uracil as described in Materials and Methods. As predicted by measurements of the rates of protein synthesis, a transient drop in total transcription characteristic of the heat shock response was seen both in mutant and wild-type strains (Fig. 3B). A significant decrease in the rate of total RNA synthesis in the mutants relative to the parental strain became apparent between 4 and 8 h. More precise measurements of the kinetics of shutoff of RNAP II activity in vivo requiring the selection of poly(A)$^+$ mRNA and correction for changes in nucleotide pool sizes are unlikely to be informative, in light of the variety of secondary metabolic changes occurring in these dying cells.

TABLE 2. Run-on transcription[a]

Yeast strain	RPO21 genotype	Radioactivity incorporated per cell[b] (10^2)			
		30°C Preshift		39°C Postshift + α-ama	
		Total	+ α-Ama[c]	8 h	16 h
YHP568	*RPO21*$^+$	8.9	4.4 (51)	1.3	0.90
YHP569	*rpo21-1*	4.7	4.3 (9)	0.84	0.56
YHP570	*rpo21-2*	4.3	3.7 (14)	1.0	0.60
YHP571	*rpo21-3*	4.2	4.1 (2)	0.75	0.50

[a] Run-on transcription reactions were performed as in the text by using cells grown at 30°C (preshift) and at the times indicated after a shift to 39°C (postshift). The assay temperature was 23°C.

[b] Values given are in counts per minute of α-[^{32}P]UMP incorporated per cell (10^2). α-Amanitin was added to the reactions indicated (+ α-ama) to a final concentration of 75 μg/ml.

[c] The numbers in parentheses indicate the percentage of total transcription at 30°C that is sensitive to inhibition by α-amanitin (RNAP II activity).

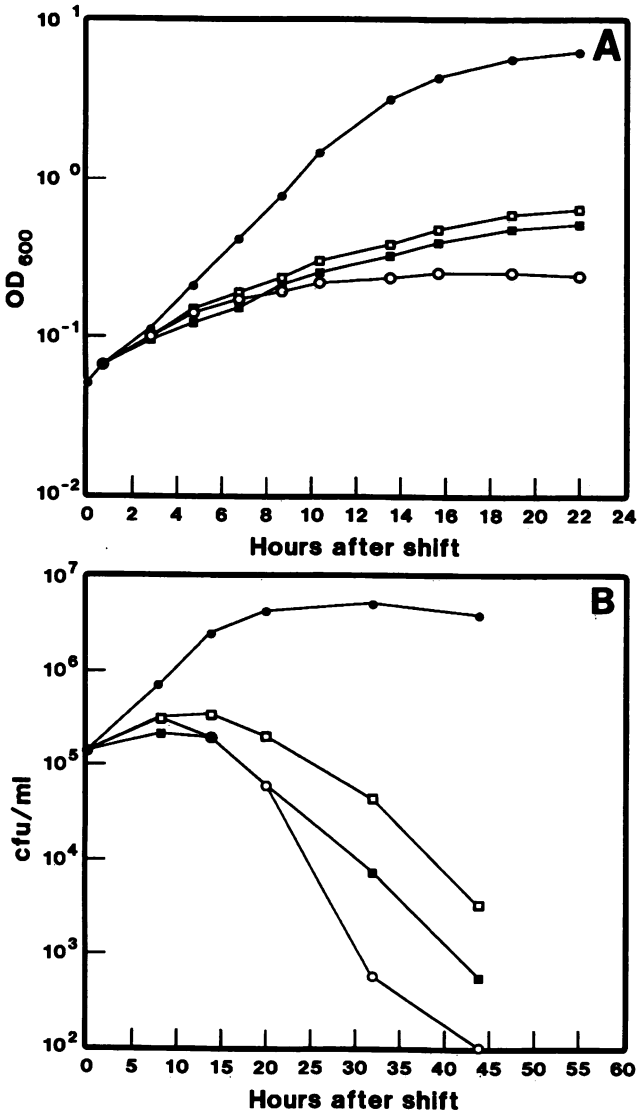

FIG. 2. Effect of incubation at 39°C on growth and viability of *rpo21* Ts⁻ mutants. (A) Cell growth, measured by increases in optical density, after a shift (at time 0) from 30 to 39°C. (B) Cell viability, measured by the ability to form colonies at 30°C, after a shift (at time 0) from 30 to 39°C. Symbols: ●, YHP568 (*RPO21*$^+$); ■, YHP569 (*rpo21-1*); ○, YHP570 (*rpo21-2*); □, YHP571 (*rpo21-3*).

In vitro RNAP activities. (i) Transcription in permeabilized cells. To obviate the need to monitor changes in nucleotide pool sizes occurring during a pulse-labeling experiment, mutant and wild-type permeabilized cells were assayed for RNA synthesis in a run-on experiment. Such run-on transcription assays have been used with tissue culture cells (34) and recently with yeast cells (13) to measure the rates of cellular RNA synthesis. RNAP II activity can be measured as the difference between total (RNAP I, II, and III) and α-amanitin-resistant (RNAP I and RNAP III) transcription (see Materials and Methods). All three mutants growing at the permissive temperature had levels of α-amanitin-resistant transcription (RNAP I and III) comparable to that of the parental strain but were almost completely deficient in α-amanitin-sensitive RNAP II activity (Table 2). Since cells were grown at the permissive temperature and assayed at 23°C, a temperature at which the *rpo21* mutants show no discernable growth defects in vivo, this lability of the enzymes may reflect fragility of all three mutant polymerases in this partially in vitro system. Perhaps the integrity of the mutant polymerases is sensitive to Sarkosyl, the detergent used to permeabilize cells before the run-on transcription assays.

To measure the response of RNAP I and III in *rpo21* mutant cells when RNAP II activity has been inhibited, α-amanitin-resistant run-on transcription (RNAP I and III) after a shift to 39°C (Table 2) was measured. The drop in activity observed in both parental and mutant cells after the temperature shift paralleled the drop in total RNA and protein synthesis rates measured in whole cells (Fig. 3). By 8 h after the shift, all three mutants showed a small, but reproducible, decline in RNAP I and III activity to approximately 70% of wild-type levels (Table 2). This decrease must be an indirect effect of the RNAP II lesions that could result, for example, from an active down-regulation of RNAP I and III activities or from the passive depletion of the mRNA pool encoding these enzyme subunits as RNAP II

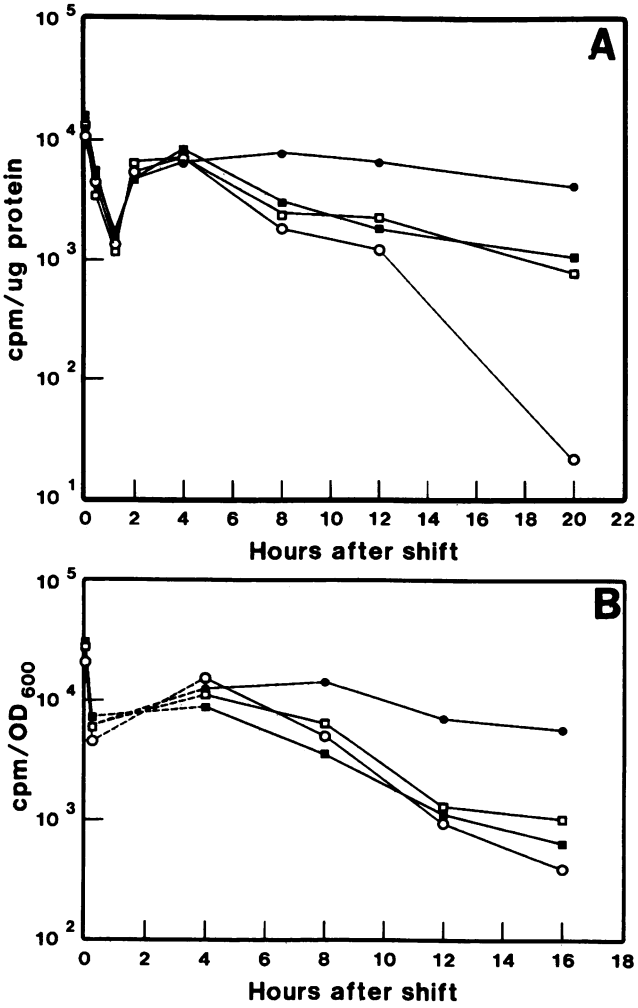

FIG. 3. Effect of incubation at 39°C on the relative rates of protein and RNA synthesis in *rpo21* mutants. (A) Protein synthesis, expressed as counts per minute per microgram of total protein in a cell extract, was measured by incorporation of L-[^{35}S]methionine during a 5-min pulse as described in Materials and Methods. (B) RNA synthesis, expressed as counts per minute per the optical density of 600 nm, was measured by incorporation of [^{3}H]uracil during a 5-min pulse as described in Materials and Methods. The kinetics of recovery of RNA synthesis in the period after a heat shock have not been determined, and thus dashed lines are used in Fig. 3B to connect 10-min and 4-h data points. Symbols: ●, YHP568 (*RPO21*$^{+}$); ■, YHP569 (*rpo21-1*); ○, YHP570 (*rpo21-2*); □, YHP571 (*rpo21-3*).

activity fails. The discrepancy between these data and the precipitous drop in the rates of total RNA synthesis shown in Fig. 3B is more apparent than real. Since the amount of radioactive precursor incorporated into RNA during a pulse in vivo is strongly influenced by equilibration of the exogenous label with the intracellular pool, the data shown in Fig. 3B overestimate the actual decrease in RNAP transcription rates. The run-on experiments do not suffer from this problem and thus reflect more accurately in vivo RNAP I and III activities.

(ii) Transcription in crude cell extracts. RNAP II and combined RNAP I and III activities can also be assayed independently in vitro in crude cell extracts. With the appropriate (empirically determined) template, ammonium sulfate concentration, and divalent cation, the assay can be made specific for either RNAP II or RNAP I and III activities (47; see Materials and Methods). S100 extracts prepared from mutant and wild-type cells were assayed for RNAP II transcription. YHP225 (*rpo21-1*) mutant cells are absolutely defective in RNAP II activity at assay temperatures ranging from 23 to 42°C (Table 3). Mixing *rpo21-1* mutant and *RPO21* extracts yielded α-amanitin-sensitive activity that was directly proportional to the amount of wild-type extract added (data not shown); thus, the *rpo21* defect was not due to increased proteolysis of RNAP II in *rpo21-1* extracts. Comparison of RNAP I and III activities (Table 3) showed no difference between YHP225 (*rpo21-1*) and the wild type; thus, the *rpo21-1* defect was, as expected, limited to RNAP II transcription. In contrast, RNAP II activity in YHP214 (*rpo21-2*) and YHP218 (*rpo21-3*) crude extracts were at wild-type (SR25-1A) levels. In an attempt to define an in vitro correlate of in vivo temperature sensitivity, the kinetics of RNAP II thermal denaturation in YHP214, YHP218, and SR25-1A extracts was measured at temperatures ranging from 23 to 65°C. Unfortunately, we were unable to discern any differences between mutant and wild-type extracts (data not shown). Interpretation of such experiments is complicated, however, by the presence of nucleases and proteases in the crude extracts, which may be activated at elevated temperatures and could mask differences in RNAP II activities.

Table 3 also shows, for comparison, assays of strain YHP225 (*rpo21-1*) transformed with the episomal plasmid pJH121, which carries the *RPO21* gene and complements the Ts^{-} phenotype in vivo. In these transformed cells growing at the permissive temperature, in vitro RNAP II (α-amanitin-sensitive) transcription was approximately 50% of wild-type levels. Since pJH121 was found in single copy in approximately 90% of cells growing under selective pressure (in uracil-omission medium; data not shown), and since the assays were done with saturating extract concentrations, these data were consistent with codominant expression of mutant and wild-type *RPO21* alleles in the transformant. The fact that a doubling of gene dosage did not result in a commensurate increase in total RNAP II activity per cell may reflect dosage compensation or limiting amounts of the other enzyme subunits.

Marker rescue and DNA sequencing. When a gapped, integrating plasmid is used to transform yeast cells, the deleted sequences are repaired during integration by using chromosomal sequences as the template (40). Mutations *rpo21-1* (strain YHP225), *rpo21-2* (strain YHP214), and *rpo21-3* (strain YHP218) were mapped by transformation with pJH124 (an integrating plasmid carrying the complete, wild-type *RPO21* gene) that had been gapped by restriction endonuclease digestion, as shown in Fig. 1B. The wild-type (Ts^{+}) *RPO21* allele can be reconstituted only if the mutation in the chromosomal gene lies outside the gapped region on the plasmid. All three Ts^{-} mutations map to the amino-terminal 1 kb of the structural gene between the *Bal*1 site at +96 and the *Tth*III1 site at +1089 (Fig. 1B), even though the mutagenized DNA fragment used to generate *rpo21* mutations comprises 3.7 kb of coding sequence (Fig. 1A).

The *Bal*1-*Tth*III1 fragment from prpo21-1, prpo21-2, and prpo21-3 was isolated and subcloned into M13mp18 for DNA sequencing and comparison to the wild-type *RPO21* sequence (1). The base pair changes in the three mutant genes are summarized in Fig. 4, along with the corresponding substitutions in the inferred amino acid sequence of the

TABLE 3. RNAP activities in crude extracts[a]

Strain	Genotype	RNAP II activity[b] at:					RNAP I + III activity[b] at 30°C
		23°C	30°C	37°C	42°C	30°C + α-ama[c]	
SR25-1A	*RPO21*⁺	1.0	1.3	0.97	0.38	0.16	0.36
YHP225	*rpo21-1*	0.14	0.12	0.13	0.10	0.12	0.34
YHP214	*rpo21-2*	1.1	1.2	0.79	0.29	0.14	0.34
YHP218	*rpo21-3*	1.0	1.2	0.92	0.40	0.15	0.35
YHP225 (pJH121)[d]	*rpo21-1* (*RPO21*⁺)	ND	0.70	ND	ND	0.16	0.33

[a] In vitro assays specific for RNAP II, or combined RNAP I and III activities, were performed as described in the text. Cells were grown at 30°C for the preparation of extracts, which were then assayed for polymerase activity at the temperatures indicated.
[b] Values given in the table are in nanomoles of GMP incorporated per milliliter of reaction mixture.
[c] α-Amanitin was added (+ α-ama) to a final concentration of 50 μg/ml.
[d] YHP225 (pJH121) is yeast strain YHP225 transformed with the *RPO21*-containing plasmid pJH121.

mutant polypeptides. The lesions found in all three *rpo21* Ts⁻ alleles lie in DNA sequence domains that are highly conserved among the largest eucaryotic RNAP subunits (1, 7; J. Corden, personal communication). In each case the most common type of nitrosoguanidine-induced nucleotide substitution has occurred, involving a GC-to-AT transition in the second of two consecutive GC base pairs (P. A. Burns, A. J. E. Gordon, and B. W. Glickman, J. Mol. Biol., in press). *rpo21-1* carries a GC-to-AT transition at nucleotide 236 corresponding to the substitution of aspartic acid (Asp) for glycine (Gly) at amino acid position 79. This glycine residue is absolutely conserved in all eucaryotic, large subunits sequenced thus far. *rpo21-2* and *rpo21-3* alleles both have a GC-to-AT transition at nucleotide 332 in the same homology domain as that of the *rpo21-1* mutation (domain I, Fig. 4), that also results in a Gly-to-Asp amino acid substitution (position 111). Since both prpo21-2 and prpo21-3 Ts⁻ transformants were derived from the same mutagenized population of plasmids, this identical change may have been due to a single mutational event. *rpo21-2*, however, harbors a second GC-to-AT transition at nucleotide 1078 in domain III (Fig. 4), corresponding to a glutamic acid-to-lysine substitution at amino acid 360 of the inferred amino acid sequence.

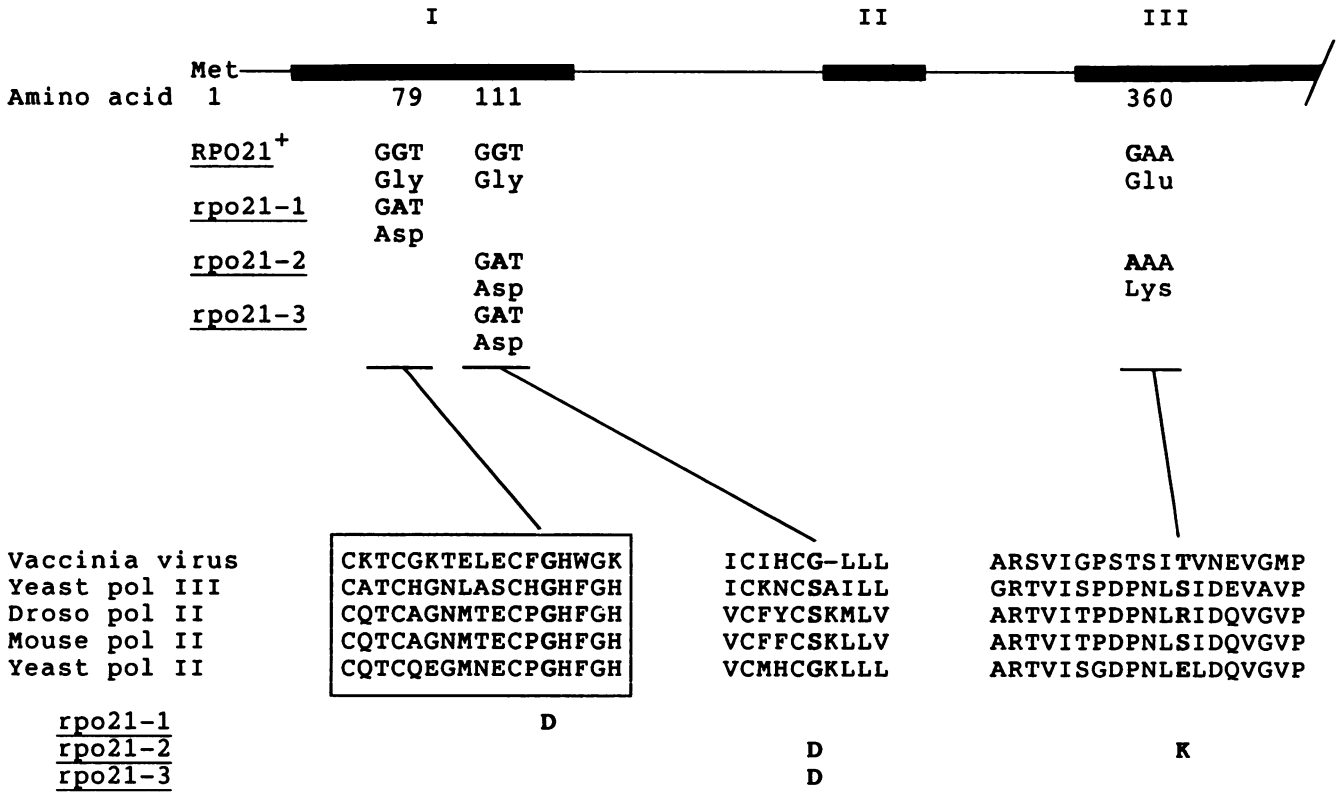

FIG. 4. DNA sequence and inferred amino acid sequence of the *rpo21* mutant genes. The amino-terminal portion of the yeast RPO21 polypeptide is indicated by a thin line, thickened sections of which delineate the homology domains I, II, and III between various RNAPs (7). The amino acid number, nucleotide sequence, and inferred amino acid are given at sites where *RPO21* and mutant (*rpo21*) DNAs differ. Using the single-letter code, the amino acids immediately surrounding the mutation sites are given for various organisms, and the putative polymerase Zn^{2+} binding site is boxed (J. Corden, personal communication). Abbreviations: Droso, *D. melanogaster*; pol, polymerase.

DISCUSSION

In the past, attempts to screen among Ts^- mutants for those defective in one specific RNAP activity in vitro have proved unsuccessful (29, 52). One *RPO21* (*RPB220*) mutant has been isolated after a screen for thiolutin sensitivity (47, 57), which, like *rpo21-1*, was absolutely defective in RNAP II activity in vitro. However, meiotic segregation analysis of this mutation (*rpob1*) revealed that the altered polypeptide and the in vitro defect did not cosegregate with any in vivo phenotype (57).

All three *rpo21* alleles studied here cause Ts^- lethality at 39°C. Measurements of cell growth, viability, and total RNA and protein synthesis showed that *rpo21-1*, *rpo21-2*, and *rpo21-3* mutations result in a delayed shutoff of RNAP II activity in cells shifted to the nonpermissive temperature. This slow shutoff phenotype of *rpo21* mutants may explain the failure of earlier attempts to identify polymerase mutants among Ts^- strains (29, 52) on the basis of their expected inability to incorporate radiolabeled precursors into RNA soon after a temperature shift. Directing mutations in a cloned *RPO21* gene to the homologous chromosomal locus has obviated the need for a RNAP II-specific phenotype in vivo as the basis for the identification of probable mutants.

Polymerase subunit mutations could impair RNAP II activity in one or both of two ways: (i) by affecting stability of the polypeptide or its assembly into holoenzyme and (ii) by affecting enzymatic function of RNAP II. The slow shutoff phenotype of *rpo21* mutants does not allow us to distinguish unambiguously between these possibilities. However, in *E. coli*, most Ts^- mutants in the homologous polymerase subunit gene (β′) are defective in subunit stability or RNAP assembly (1, 18, 27) and do show a slow shutoff of RNA synthesis after a temperature shift. Also, the temperature-independent defect of RNAP II in *rpo21-1* S100 extracts and of all three mutant polymerases when assayed in permeabilized cells is consistent with assembly or stability mutants that are fragile outside the intact cell.

One explanation of the slow shutoff phenotype might be that mutant polymerases assembled at 30°C continue to function after a temperature shift. Thus, the eventual drop in RNAP II activity could simply be the result of a block to the assembly of polymerase holoenzyme at the restrictive temperature and the consequent dilution of the preexisting cellular pool of RNAP II as cells divide; during this time the cell number has increased two- to threefold. If the mutations are not leaky and block assembly of holoenzyme immediately after the temperature shift, then our observations suggest excess RNAP II capacity in cells growing vegetatively at 30°C.

The complete absence of RNAP II in vitro activity in S100 extracts of *rpo21-1* provides a useful marker for monitoring enzyme activity levels in vivo. For example, in vitro RNAP II activity is approximately 50% of wild-type levels in extracts prepared from merodiploid *rpo21-1* transformants, which harbor a wild-type *RPO21* gene on an episome (pJH121), when these cells are grown at 30°C. Thus it appears that at the permissive temperature, mutant and wild-type *RPO21* polypeptides are codominantly expressed and assembled with equal efficiency into a RNAP II holoenzyme.

The isolation and characterization of *rpo21* mutants can provide valuable clues concerning the relevance of evolutionarily conserved DNA sequence domains to polymerase subunit function in vivo. In ths regard, it is interesting that, while our method of mutagenesis was random, a biological screen for perturbations in *RPO21* function (a Ts^- phenotype) has yielded three mutants, all of which lie within conserved homology regions. Mutants *rpo21-2* and *rpo21-3* both have substitutions at position +111 in homology domain I, while *rpo21-2* harbors an additional Glu-to-Lys change at position +360 in domain III (Fig. 4). The additional amino acid substitution in this mutant, versus *rpo21-3*, must therefore be responsible for the increased thermosensitivity of *rpo21-2* strains. Homology domain III has been suggested on the basis of homology to *E. coli* DNA polymerase I to encode a DNA-binding helix-turn-helix motif (1, 38). The second mutation (+360) in mutant *rpo21-2* lies in one of these proposed helix regions (38). Perhaps this mutation impairs the DNA-binding properties of RNAP II; *E. coli* RNAP subunit β′ has been implicated in DNA binding (16). Finally, the alteration in *rpo21-1* is at amino acid position +79 and lies not only in the first conserved domain (Fig. 4), but also within a possible metal-binding subdomain (2, 35) whose sequence is highly conserved in the largest subunits of RNAP II of *S. cerevisiae*, *D. melanogaster*, and mouse cells (Fig. 4; J. Corden, personal communication). A tightly bound Zn^{2+} atom is found in purified preparations of RNAP II from a wide variety of cell types (14, 30, 43) and is thought to be essential for enzyme activity and perhaps holoenzyme integrity (54). One hypothesis under investigation is that the *rpo21-1* lesion may act by reducing the affinity of the mutant subunit for Zn^{2+}.

ACKNOWLEDGMENTS

We thank Jacqueline Segall, Jacques Archambault, Deborah Field, Sara Petersen-Bjørn, and Keith Schappert for comments.

This work was funded by the Medical Research Council of Canada and the Natural Sciences and Engineering Research Council of Canada. H.J.H. was the recipient of a Medical Research Council studentship. E.M.S. was the recipient of a Medical Research Council fellowship.

LITERATURE CITED

1. **Allison, L. A., M. Moyle, M. Shales, and C. J. Ingles.** 1985. Extensive homology among the largest subunits of eukaryotic and prokaryotic RNA polymerases. Cell **42**:599–610.
2. **Berg, J. M.** 1986. Potential metal-binding domains in nucleic acid binding proteins. Science **232**:485–487.
3. **Biggs, J., L. Searles, and A. L. Greenleaf.** 1985. Structure of the eukaryotic transcription apparatus: features of the gene for the largest subunit of *Drosophila* RNA polymerase II. Cell **42**:611–621.
4. **Boeke, J. D., F. LaCroute, and G. R. Fink.** 1984. A positive selection for mutants lacking orotidine-5′-phosphate decarboxylase activity in yeast: 5-fluoro-orotic acid resistance. Mol. Gen. Genet. **197**:345–346.
5. **Bradford, M. M.** 1976. A rapid and sensitive method for the quantitation of microgram quantities of protein utilizing the principle of protein dye binding. Anal. Biochem. **72**:248–254.
6. **Breant, B., J. Huet, A. Sentenac, and P. Fromageot.** 1983. Analysis of yeast RNA polymerases with subunit-specific antibodies. J. Biol. Chem. **258**:11968–11973.
7. **Broyles, S. S., and B. Moss.** 1986. Homology between RNA polymerases of poxviruses, prokaryotes, and eukaryotes: nucleotide sequence and transcriptional analysis of vaccinia virus genes encoding 147-kDa and 22-kDa subunits. Proc. Natl. Acad. Sci. USA **83**:3141–3145.
8. **Buhler, J.-M., J. Huet, K. E. Davies, A. Sentenac, and P. Fromageot.** 1980. Immunological studies of yeast nuclear RNA polymerases at the subunit level. J. Biol. Chem. **255**:9949–9954.
9. **Chan, V. L., G. F. Whitmore, and L. Siminovitch.** 1972. Mammalian cells with altered forms of RNA polymerase II. Proc. Natl. Acad. Sci. USA **69**:3119–3123.

10. **Cho, K. W. Y., K. Khalili, R. Zandomeni, and R. Weinmann.** 1985. The gene encoding the large subunit of human RNA polymerase II. J. Biol. Chem. **28**:15204–15210.
11. **Davis, R. W., M. Thomas, J. Cameron, T. P. St. John, and R. A. Padgett.** 1980. Rapid DNA isolations for enzymatic and hybridization analysis. Methods Enzymol. **65**:404–411.
12. **Dente, L., G. Cesareni, and R. Cortese.** 1983. pEMBL: a new family of single stranded plasmids. Nucleic Acids Res. **11**: 1645–1655.
13. **Elion, E. A., and J. R. Warner.** 1986. An RNA polymerase I enhancer in *Saccharomyces cerevisiae*. Mol. Cell. Biol. **6**: 2089–2097.
14. **Falchuk, K. H., B. Mazus, L. Ulpino, and B. L. Vallee.** 1976. *Euglena gracilis* DNA dependent RNA polymerase II: a zinc metalloenzyme. Biochemistry **15**:4468–4475.
15. **Friesen, J. D., M. Tropak, and G. An.** 1983. Mutations in the *rplJ* leader of *Escherichia coli* that abolish feedback regulation. Cell **32**:361–369.
16. **Fukuda, R., and A. Ishihama.** 1974. Subunits of RNA polymerase in function and structure. V. Maturation *in vitro* of core enzyme from *Escherichia coli*. J. Mol. Biol. **87**:523–540.
17. **Greenleaf, A. L., L. M. Borsett, P. F. Jiamachello, and D. E. Coulter.** 1979. α-Amanitin-resistant *D. melanogaster* with an altered RNA polymerase II. Cell **18**:613–622.
18. **Gross, C., D. A. Fields, and E. K. F. Bautz.** 1976. Characterization of a ts B′ mutant RNA polymerase of *Escherichia coli*. Mol. Gen. Genet. **147**:337–341.
19. **Guialis, A., K. E. Morrison, and C. J. Ingles.** 1979. Regulated synthesis of RNA polymerase II polypeptides in Chinese hamster ovary cell lines. J. Biol. Chem. **254**:4171–4176.
20. **Himmelfarb, H. J., E. Maicas, and J. D. Friesen.** 1985. Isolation of the *SUP45* omnipotent suppressor gene of *Saccharomyces cerevisiae* and characterization of its gene product. Mol. Cell. Biol. **5**:816–822.
21. **Hinnen, A., J. B. Hicks, and G. R. Fink.** 1978. Transformation of yeast. Proc. Natl. Acad. Sci. USA **75**:1929–1933.
22. **Huet, J., A. Sentenac, and P. Fromageot.** 1982. Spot-immunodetection of conserved determinants in eukaryotic RNA polymerases. J. Biol. Chem. **257**:2613–2618.
23. **Ingles, C. J.** 1978. Temperature-sensitive RNA polymerase II mutations in Chinese hamster ovary cells. Proc. Natl. Acad. Sci. USA **75**:405–409.
24. **Ingles, C. J., H. J. Himmelfarb, M. Shales, A. L. Greenleaf, and J. D. Friesen.** 1984. Identification, molecular cloning, and mutagenesis of *Saccharomyces cerevisiae* RNA polymerase genes. Proc. Natl. Acad. Sci. USA **81**:2157–2161.
25. **Ito, H., Y. Fukuda, K. Murata, and A. Kimura.** 1983. Transformation of intact yeast cells treated with alkali cations. J. Bacteriol. **153**:163–168.
26. **Kedinger, C., M. Gniazolowski, J. L. Mandel, Jr., F. Gissinger, and P. Chambon.** 1970. α-Amanitin: a specific inhibitor of one of two DNA-dependent RNA polymerase activites from calf thymus. Biochem. Biophys. Res. Commun. **38**:165–171.
27. **Kirschbaum, J. B.** 1976. A bacterial mutant which overproduces the β and β′ subunits of *Escherichia coli* RNA polymerase, p. 67–83. *In* N. C. Kjeldgaard and O. Maaløe (ed.), Control of ribosome synthesis. Alfred Benzon Symposium IX. Munksgaard International Publishers, Ltd., Copenhagen.
28. **Klapholz, S., and R. E. Esposito.** 1982. A new mapping method employing a meiotic rec⁻ mutant of yeast. Genetics **100**: 382–412.
29. **Lacroute, F., J. Huet, and F. Exinger.** 1975. Dominant and semidominant mutations leading to thermosensitivity of ribonucleic acid biosynthesis in *Saccharomyces cerevisiae*. J. Bacteriol. **122**:847–854.
30. **Lattke, H., and U. Weser.** 1976. Yeast RNA-polymerase B: a zinc protein. FEBS Lett. **65**:288–292.
31. **Lindell, T. J., F. Weinberg, P. W. Morris, R. G. Roeder, and W. J. Rutter.** 1970. Specific inhibition of nuclear RNA polymerase II by α-amanitin. Science **170**:447–449.
32. **Lindquist, S.** 1986. The heat-shock response. Annu. Rev. Biochem. **55**:1151–1191.
33. **Maniatis, T., E. F. Fritsch, and J. Sambrook.** 1982. Molecular cloning: a laboratory manual. Cold Spring Harbor Laboratory, Cold Spring Harbor, N.Y.
34. **McKnight, G. S., and R. D. Palmiter.** 1979. Transcriptional regulation of the ovalbumin and conalbumin genes by steroid hormones in chick oviduct. J. Biol. Chem. **254**:9050–9058.
35. **Miller, J., A. D. McLachlan, and A. Klug.** 1985. Repetitive zinc-binding domains in the protein transcription factor IIIA from *Xenopus* oocytes. EMBO J. **4**:1609–1614.
36. **Miller, M. J., N.-H. Xuong, and E. P. Geiduschek.** 1979. A response of protein synthesis to temperature shift in the yeast *Saccharomyces cerevisiae*. Proc. Natl. Acad. Sci. USA **76**: 5222–5225.
37. **Miller, M. J., N.-H. Xuong, and E. P. Geiduschek.** 1982. Quantitative analysis of the heat shock response of *Saccharomyces cerevisiae*. J. Bacteriol. **151**:311–327.
38. **Ollis, D. L., P. Buck, R. Hamlin, N. G. Xuong, and T. A. Steitz.** 1985. Structure of the large fragment of *Escherichia coli* DNA polymerase I complexed with dTMP. Nature (London) **313**: 762–766.
39. **Orr-Weaver, T. L., and J. W. Szostak.** 1983. Multiple, tandem plasmid integration in *Saccharomyces cerevisiae*. Mol. Cell. Biol. **3**:747–749.
40. **Orr-Weaver, T., J. W. Szostak, and R. J. Rothstein.** 1981. Yeast transformation: a model system for the study of recombination. Proc. Natl. Acad. Sci. USA **78**:6354–6358.
41. **Ovchinnikov, Y. A., G. S. Monatyrskaya, V. V. Gubanov, S. O. Guryev, I. S. Salomatina, T. M. Shuvaeva, V. M. Lipkin, and E. D. Sverdlov.** 1982. The primary structure of *E. coli* RNA polymerase. Nucleotide sequence of the rpoC gene and amino acid sequence of the β′-subunit. Nucleic Acids Res. **10**:4035–4044.
42. **Percival-Smith, A., and J. Segall.** 1986. Characterization and mutational analysis of a cluster of three genes expressed preferentially during sporulation of *Saccharomyces cerevisiae*. Mol. Cell. Biol. **6**:2443–2451.
43. **Petranyi, P., J. J. Jendrisak, and R. R. Burgess.** 1977. RNA polymerase II from wheat germ contains tightly bound zinc. Biochem. Biophys. Res. Commun. **74**:1031–1038.
44. **Riva, M., S. Memet, J.-Y. Micouin, J. Huet, I. Treich, J. Dassa, R. Young, J.-M. Buhler, A. Sentenac, and P. Fromageot.** 1986. Isolation of structural genes for yeast RNA polymerases by immunological screening. Proc. Natl. Acad. Sci. USA **83**:1554–1558.
45. **Roeder, R. G.** 1976. Eukaryotic nuclear RNA polymerase, p. 285–329. *In* R. Losick and M. Chamberlin (ed.), RNA polymerase. Cold Spring Harbor Laboratory, Cold Spring Harbor, N.Y.
46. **Ruet, A., A. Sentenac, and P. Fromageot.** 1978. A specific assay for yeast RNA polymerases in crude cell extracts. Eur. J. Biochem. **90**:325–330.
47. **Ruet, A., A. Sentenac, P. Fromageot, B. Winsor, and F. Lacroute.** 1980. A mutation of the B_{220} subunit gene affects the structural and functional properties of yeast RNA polymerase B *in vitro*. J. Biol. Chem. **255**:6450–6455.
48. **Sanger, F., S. Nicklen, and A. R. Coulson.** 1977. DNA sequencing with chain terminating inhibitors. Proc. Natl. Acad. Sci. USA **74**:5463–5467.
49. **Schultz, L. D., and B. D. Hall.** 1976. Transcription in yeast: α-amanitin sensitivity and other properties which distinguish between RNA polymerase I and III. Proc. Natl. Acad. Sci. USA **73**:1029–1031.
50. **Searles, L. L., R. S. Jokerst, P. M. Bingham, R. A. Voelker, and A. L. Greenleaf.** 1982. Molecular cloning of sequences from a *Drosophila* RNA polymerase II locus by P element transposon tagging. Cell **31**:585–592.
51. **Shortle, D., P. Novick, and D. Botstein.** 1984. Construction and genetic characterization of temperature-sensitive mutant alleles of the yeast actin gene. Proc. Natl. Acad. Sci. USA **81**:4889–4893.
52. **Thonart, P., J. Bechet, F. Hilger, and A. Burny.** 1976. Thermosensitive mutations affecting ribonucleic acid polymerases in *Saccharomyces cerevisiae*. J. Bacteriol. **125**:25–32.
53. **Valenzuela, P., G. Hager, F. Weinberg, and W. J. Rutter.** 1976. Molecular structure of yeast RNA polymerase III: demonstra-

tion of the tripartite transcriptive system in lower eucaryotes. Proc. Natl. Acad. Sci. USA **73**:1024–1028.
54. **Valenzuela, P., R. W. Morris, A. Faras, W. Levinson, and W. J. Rutter.** 1973. Are all nucleotidyl transferases metalloenzymes? Biochem. Biophys. Res. Commun. **53**:1036–1041.
55. **Vieira, J., and J. Messing.** 1982. The pUC plasmids, and M13mp7-derived system for insertion mutagenesis and sequencing with synthetic universal primers. Gene **19**:259–268.
56. **Weeks, J. R., D. E. Coulter, and A. L. Greenleaf.** 1982. Immunological studies of RNA polymerase II using antibodies to subunits of *Drosophila* and wheat germ enzyme. J. Biol. Chem. **257**:5884–5891.
57. **Winsor, B., and F. Lacroute.** 1979. Isolation and characterisation of a strain of *Saccharomyces cerevisiae* deficient in *in vitro* polymerase B(II) activity. Mol. Gen. Genet. **173**:145–151.
58. **Yanisch-Perron, C., J. Vieira, and J. Messing.** 1985. Improved M13 phage cloning vectors and host strains: nucleotide sequences of the M13mp18 and pUC19 vectors. Gene **3**:103–119.